Novel high entropy alloys as binder in cermets: from design to sintering

E. Prieto[a*], A. Vaz-Romero[b] J. Gonzalez-Julian[c], R. de Oro[d], S. Guo[e], P. Alvaredo [a]

[a]Materials science and engineering and chemical engineering department, IAAB, Universidad Carlos III de Madrid, Avda. Universidad, 30, 28911 Leganés, Madrid, Spain.
[b]Continuum Mechanics and Structural Analysis Universidad Carlos III de Madrid, Avda. Universidad, 30, 28911 Leganés, Madrid, Spain.
[c]Institute of Energy and Climate Research (IEK-1) Forschungszentrum Jülich GmbH (IEK-1), 52425 Jülich, Germany
[d]Institute of Chemical Technologies and Analytics. Vienna University of Technology. Getreidemarkt 9/164, A 1060 Vienna, Austria
[e]Department of Industrial and Materials Science, Chalmers University of Technology, SE-412 96, Göteborg, Sweden
* paula.alvaredo@uc3m.es

Abstract

In recent years a new group of alloys has emerged breaking with the classical alloying concepts of physical metallurgy, high entropy alloys (HEA). Their main characteristic is that these alloys present 4 or 5 main elements increasing the entropy of the system and favouring the formation of a single phase: a disordered solid solution formed by all involved alloying elements giving way to an alloy with high thermal stability, hardness and strength. These properties make this group of alloys attractive as candidates for alternative binders in hard materials. In this work, two new compositions have been designed with the aim of obtaining a single BCC phase, reducing the cost and minimizing the presence of critical elements using elements that can present good potential properties for a cermet and with low toxicity and price such as Al, Cr, Mo, Ni, Fe and Ti. The design has been made based on the composition calculation applying the HEA phase formation empirical rules from literature in combination with thermodynamic simulations by Calphad method. The viability of the compositions has been studied through the processing of the compositions by casting and the study of wettability and solubility at high temperature on the hard phase of TiCN. Once the chosen compositions have been validated as competitive binders, cermets have been consolidated by spark plasma sintering (SPS) and the influence of the compositions on the mechanical properties of the compound materials has been studied.

Keywords
High entropy alloys, HEA, composition design, cermets, alternative binders, Spark Plasma Sintering

Highlights

- Design of new HEAs intended as alternative binders
- Study of wetting between HEA binders and TiCN hard phase
- Influence of HEA composition on mechanical properties of the cermets
- New alloy as binder avoiding critical elements

1. Introduction

Nowadays, one of the main research lines in the field of hard materials is the development of new compositions of binders. In the literature some works can be found investigating new binder compositions for cemented carbides, cermets and polycrystalline diamond (PCD). The main reasons that drive the search for new metallic binders are diverse, firstly the need to find alloys cheaper, less toxic and more environmentally friendly than conventional Co and Ni [1] and, secondly, to apply knowledge in metal alloys to design compositions *ad hoc* for each cutting and forming operation. The most promising metal for complete or partial substitution of Co and Ni in hardmetals and cermets is

Fe, due to their lower price and toxicity in addition to their high versatility, as a result of the great industrial knowledge of this metal [2]. Particularly in the bibliography there are some works which study in depth the sintering mechanism of Fe-based / TiCN cermets and the influence of the binder composition and the consolidation method on the final properties of the metal-ceramic material. [3, 4]. However, the successful application of Fe-based alloys as binder in hard materials requires overcoming some technological difficulties as the phase change in service, the obtention of full density parts and the improvement of wear and corrosion resistance.

The objective of the present work is to investigate new compositions as binder that present a high phase stability minimizing the number of phases present in the compound material, thus avoiding phase changes in service and facilitating industrial production. In this way, high entropy alloys (HEAs) are postulated as good candidates to act as alternative binders [5-9]. This young group of alloys began to develop in 2004 and present very attractive characteristics that are given by the nature of their compositions. Originally, within this group of alloys, those with a minimum of 5 elements in equimolar proportion were considered, however, today HEA is considered to be those compositions that give rise to high entropy, even considering alloys with up to 3 elements that do not present a similar atomic percentage. All these alloys have in common that their thermodynamic properties give rise to a lower number of phases than that predicted by the Gibbs phase rule, giving rise to alloys with a single-phase microstructure that presents high stability (Equation 1) [10].

$$\Delta G_{mix} = \Delta H_{mix} - T\Delta S_{mix} \qquad \text{Equation 1}$$

It is possible to determine if the phase formed in the alloy is an amorphous phase, an intermetallic compound or a solid solution by playing with the elements and their proportion since the nature of the alloy phase structure will be determined by the characteristics of the involved elements. Based on the numerous experimental dataset of HEAs, the influence factors on the phase stability can be studied from the perspective of mixing enthalpy, electronegativity difference, valence electron concentration and atomic size difference [11]. The values of these thermodynamic, physical and chemical parameters will determine the formation of a simple solid solution rather than amorphous phases or intermetallic compounds.

Obtaining a simple solid solution results in surprising properties. The different nature of the elements in the solid solution results in a severe lattice distortion which not only increases the mechanical properties but also decreases the thermal effect on them. Also, the severe lattice distortion results in a low diffusion kinetic which is the responsible of the characteristic properties of these alloys as high thermal stability, inhibition of grain growth and formation of nano-precipitates. These characteristics make these alloys attractive for a wide range of applications, one of them being the possibility to be alternative binders in hard materials. The studied HEA compositions as alternative binder in cermets found in the literature are from the family of Cantor´s alloy all of them with a face centered cubic (FCC) crystalline structure: CoCrFeNi [5], CoCrFeNiCu [6,7], FeCoNi [8], FeCoCrNiAl [9]. The authors report an increase in hardness, oxidation resistance, fracture toughness and wear resistance as compared with cermets with conventional binders at room and high temperature due to the fact that HEA binders inhibit the growth of core rim grains and lead to finer microstructures due to the sluggish diffusion effect.

This work proposes two new HEA compositions and explore their capability to be alternative binders in cermets. The study comprises four stages: i) Composition design; ii) Composition validation; iii) Cermet manufacturing; and iv) Mechanical properties evaluation. Two different high entropy alloys have been designed in order to obtain a simple solid solution with a body centered cubic (BCC) crystalline structure. The reason why this crystalline structure has been chosen is because BCC alloys show higher hardness and it has the crystalline structure of the Fe-based binders studied before. The elements that have been used in the design of the compositions are those that can provide the characteristics that are required in a tool material, reducing the cost and weight of the alloy and avoiding the presence of refractory metals that can hinder their processing. The design of the crystalline phase of the two compositions has been carried out by studying the physicochemical properties of the involved elements and by calculating their phase diagram by thermodynamic simulation.

Subsequently, the compositions design has been validated by processing the characterization of cast samples with the three compositions. Once the crystalline phase formed has been verified, its viability as an alternative binder in cermets has been studied by analysing the high temperature interaction of each alloy on TiCN. The processing of these alloys is performed by liquid phase sintering (LPS) and its success lies in the sintering mechanism which involves the

dissolution of the hard phase particles by the molten binder. So, the success of the processing goes through the wetting and solubility behaviour between the binder and the hard phase particles [12]. Those compositions that meet the characteristics of solubility and wetting with the Ti(C, N) substrate will be processed by powder metallurgy. The HEA powder will be obtained by gas atomization and cermets with the new binder compositions will be consolidated by spark plasma sintering (SPS). Hardness and compressive test are performed and compared with conventional cermets in order to determine the viability of the cermets with the new binder composition and the influence of the composition in the mechanical behaviour.

2. Experimental procedure

In this work, two different high entropy alloys of 5 and 6 elements have been designed in order to obtain a single phase solid solution with a BCC crystalline structure and the elements have chosen with the aim to minimize the density of the cermet and the use of critical elements to later evaluate their viability as a binder in cermets. The design has been performed by the calculations of the thermodynamic properties of the alloys using the equations 2-6, supporting the results by the calculation of their equilibrium phase diagrams. Equilibrium phase diagrams were calculated using the Thermo-Calc software. Calculations are based on the free Gibbs energy minimization code and mass conversion rule, in combination with TCFE7 and TTNI7 databases (Scientific Group Thermodata Europe).

$$\Delta S_{mix} = -R \sum_{i=1}^{n} c_i \ln c_i \qquad \text{Equation 2}$$

Where R is the gas constant and c_i is the mole percent of ith component.

$$\Delta H_{mix} = \sum_{i=1, i\neq j}^{n} \Delta H_{ij}\, c_i c_j \qquad \text{Equation 3}$$

Where c_i and c_j are the atomic percentage of the ith or jth component and ΔH_{ij} is the mixing enthalpy of the binary liquid alloy.

$$\Delta\chi = \sqrt{\sum_{i=1}^{n} c_i}\ \left(\chi_i - \chi_{avg}\right)^2;\ \chi_{avg} = \sum_{i=1}^{n} c_i \chi_i \qquad \text{Equation 4}$$

Where c_i is the atomic percentage and χ_i is the Pauling electronegativity for the ith element.

$$\delta = \sqrt{\sum_{i=1}^{n} c_i}\left(1 - \frac{r_i}{r_{avg}}\right)^2;\ r_{avg} = \sum_{i=1}^{n} c_i r_i \qquad \text{Equation 5}$$

Where c_i is the atomic percentage and $r_i$the atomic radius of the ith element.

$$VEC = \sum_{i=1}^{n} c_i\, VEC_i \qquad \text{Equation 6}$$

Where c_i is the atomic percentage of the ith element and VEC_i is the VEC of the ith element.

Cast samples of the designed compositions have been prepared by arc-melting of a mixture of powders of the constituent elements with purity better than 99.9 % in a Ti-gettered high-purity Ar atmosphere. Repeated melting has been carried out at least five times to improve the chemical homogeneity of the alloy. The molten alloy has been drop-cast into a 10 mm diameter copper mold. The characterization of the casted samples has been carried out by microstructural observation in a scanning electron microscope FE-SEM TENEO. The phase formation of the cast samples has been studied by X-ray diffraction in a Phillips equipment X'Pert-MPD and the data were processed using the X'Pert Highscore software.

To study the wetting behavior of three new alloys on Ti (C,N) ceramic substrates wetting experiments up to 1600 °C were performed. The temperature of the wetting experiments will be determined for the thermal behavior of the alloy which will be analyzed by differential thermal analysis (DTA) in a SETARAM equipment (SETSYS Evolution 16/18). The analyses were performed in an Al_2O_3 crucible under Ar (99.999 %) atmosphere up to 1500 °C at 20 °C/min.

Wetting experiments were conducted in a tube furnace under Ar atmosphere. The furnace is provided with a camera to record the metal melting and the formation of the liquid metal drop, as well as its evolution with time. So, the evolution of the contact angle between the two phases with respect to the residence time and temperature was monitored by the sessile drop method, taking as t = 0 the moment at which the melting of the metal sample is started. A small piece of the HEA cast sample is placed on the $Ti(C_{0.5}N_{0.5})$ substrate. This substrate is sintered from $Ti(C_{0.5}N_{0.5})$ powders (H. C. Stark, ρ = 5.12 g/cm^3; D50 = 3.71 µm) by spark plasma sintering (SPS) at 1900 °C and 70 MPa with a heating and cooling rate of 200 K/min. This consolidation technique is chosen to achieve a dense substrate with minimal porosity in order to evaluate the wetting behavior and avoid the infiltration of the liquid metal. The density of the sintered $Ti(C_{0.5}N_{0.5})$ substrates is 99.3 %. To study the interface formed between the metal alloy and the ceramic substrate after the wetting experiment, the metallographic preparation is carried out on the cross-sectional surface and the microstructure is studied using scanning electron microscopy, analyzing the composition using EDX.

After analyzing the results obtained in the wetting experiments, the viable compositions are selected to be binder in cermets and the compound materials are processed using spark plasma sintering (SPS). To do this, the powders of the HEA designed compositions are obtained by gas atomization with an outlet pressure of 41 ± 1.7 bar under Ar atmosphere. The characterization of the atomized powders was performed using the following techniques: oxygen analysis by inert gas fusion technique by LECO, density measurement by He pycnometry, morphology and composition study by scanning electron microscopy (SEM) with an energy dispersive spectrometer (EDS), and phase identification by X-ray diffraction (XRD). The HEA atomized powders are mixed in a Turbula® with the $Ti(C_{0.5}N_{0.5})$ powders (H. C. Stark, ρ = 5.12 g/cm^3; D50 = 3.71 µm) in 20 ml of EtOH 99 % purity during 12 hours in a ratio of 50/50 vol. %. (This high percentage of binder phase is chosen to compare the behaviour of these new binder compositions with others works with alternative binders of the author [13, 14]). The ball-powder ratio was 10:1. Afterwards, it is dried on the rotary evaporator for 1 hour and then in a furnace during 30 min at 70 °C to ensure that the powders are free of moisture.

Spark plasma sintering (SPS) was used to consolidate the atomized powders. SPS was carried out in a Field Assisted Sintering Technology/Spark Plasma Sintering (FAST/SPS, FCT-HPD5, FCT Systeme GmbH, Germany) under reduced pressure (~4 mbar) to avoid oxygen enrichment during the whole thermal cycle. Temperature was controlled using a pyrometer that was focused on the surface of a drilled punch at only 5 mm from the powder. After the densification process, the surfaces of the samples were ground to eliminate the remaining graphite. To protect the tool, an additional graphite foil was placed between the powder and the graphite punches. The atomized powders were added into a graphite die of 20 mm diameter and sintered at 1300 °C during 1s at 100 K/min under a pressure of 50 MPa. These conditions were chosen after a previous study of holding time and heating rate influence on microstructure and properties of the sintered cermets. The density of the samples was measured by Archimedes method and the relative density has been calculated taking the density measured by dimensions and weight of the sample as theoretical density.

The microhardness measurements were performed by Zwick-Roell ZHµ HD microhardness tester. Quasi-static compression tests were conducted using a servo-hydraulic testing machine INSTRON 8516 100kN under displacement control. In all the experiments, the axial engineering strain in the specimen is calculated relying on the data provided by a LVDT Deflection Sensor mounted directly on the surface of the compression platens. The contact interfaces of the samples were lubricated using molybdenum disulfide grease. Experiments were conducted at a nominal (initial) strain rate of $\dot{\varepsilon}_0 = 10^{-3}s^{-1}$ at room temperature

3. Results

3.1. Designing new HEA compositions

To design the new HEA composition the elements selection has been performed with the aim to provide the characteristics required in a tool material, reducing the cost and weight of the alloy and avoiding the presence of refractory metals that can hinder their processing. The proportion of each element in the alloy has been adjusted in the alloy formulation to achieve the physical-chemical properties that give rise to the formation of a single solid solution with a body centered cubic (BCC) crystalline structure according to the ranges established in the bibliography. There are some theories about the rules of phase formation and most of them state that solid solution is formed when enthalpy of mixing (ΔH_{mix}) is slightly positive or not enough negative and when atomic size (δ) is small, and entropy of mixing (ΔS_{mix}) is high. Valence electron concentration (VEC) also has a weak effect on the phase formation, however plays a decisive role in determining the crystalline structure of the solid solution, FCC or BCC, which will determine the final mechanical properties of the alloy. In this work the theories found in the bibliography have been taken into

account to design the alloy compositions and the selected elements have been Fe, Cr, Al, Ti, Mo and Ni because because they are the potentially suitable candidates to provide the required properties in a cermet. The final designed alloys are: $Fe_{1.5}Cr_1Al_{0.75}Mo_{0.1}Ti_{0.1}$ and $Fe_{1.5}Cr_1Al_{0.75}Mo_{0.1}Ti_{0.1}Ni_{0.25}$ whose nominal compositions are shown in Table 1. The compositions have been designed so that their physicochemical properties are within the ranges: $0 \leq \delta \leq 6.6$ (%); $-22 \leq \Delta H_{mix} \leq 7$ (kJ/mol) and $10 \leq \Delta S_{mix} \leq 19.5$ (J/K·mol) and VEC < 6.87 [15-18]. The physicochemical properties of the alloys are shown in Table 2.

Table 1. Nominal composition of the designed alloys $Fe_{1.5}Cr_1Al_{0.75}Mo_{0.1}Ti_{0.1}$ (HEA-5) and $Fe_{1.5}Cr_1Al_{0.75}Mo_{0.1}Ti_{0.1}Ni_{0.25}$ (HEA-6).

HEA-5	Fe	Cr	Al	Mo	Ti	Ni
% wt.	49.1	30.6	11.9	5.6	2.8	-
% at.	43.4	29.0	21.7	2.9	2.9	-
HEA-6	Fe	Cr	Al	Mo	Ti	Ni
% wt.	45.4	28.2	11.0	4.8	2.6	8.0
% at.	40.6	27.1	20.3	2.5	2.7	6.8

Table 2. Physicochemical properties of the HEA designed compositions.

	ΔS_{mix} (kJ/mol)	ΔH_{mix}(kJ/mol)	δ (%)	Δχ	VEC
$Fe_{1.5}Cr_1Al_{0.75}Mo_{0.1}Ti_{0.1}$ (HEA-5)	10.52	-9.38	6.44	0.12	6.14
$Fe_{1.5}Cr_1Al_{0.75}Mo_{0.1}Ti_{0.1}Ni_{0.25}$ (HEA-6)	11.96	-10.44	6.30	0.13	6.42

The designed HEA compositions has been supported by the calculation of the equilibrium phase diagrams of the designed alloys, $Fe_{1.5}Cr_1Al_{0.75}Mo_{0.1}Ti_{0.1}$ (HEA-5) and $Fe_{1.5}Cr_1Al_{0.75}Mo_{0.1}Ti_{0.1}Ni_{0.25}$ (HEA-6) using Thermo-Calc software and they are shown in Figure 1. The diagrams have been represented as a function of Ti molar percentage and the content of the other elements present in the alloy has been fixed. The molar content of Ti in the respective alloys is pointed by a vertical dotted line. The equilibrium phase diagrams of the alloy FeCrAlTiMo (HEA-5) and FeCrAlTiMoNi (HEA-6) equilibrium phase diagrams show the formation of only one phase with crystalline structure BCC at room temperature as it has been predicted before.

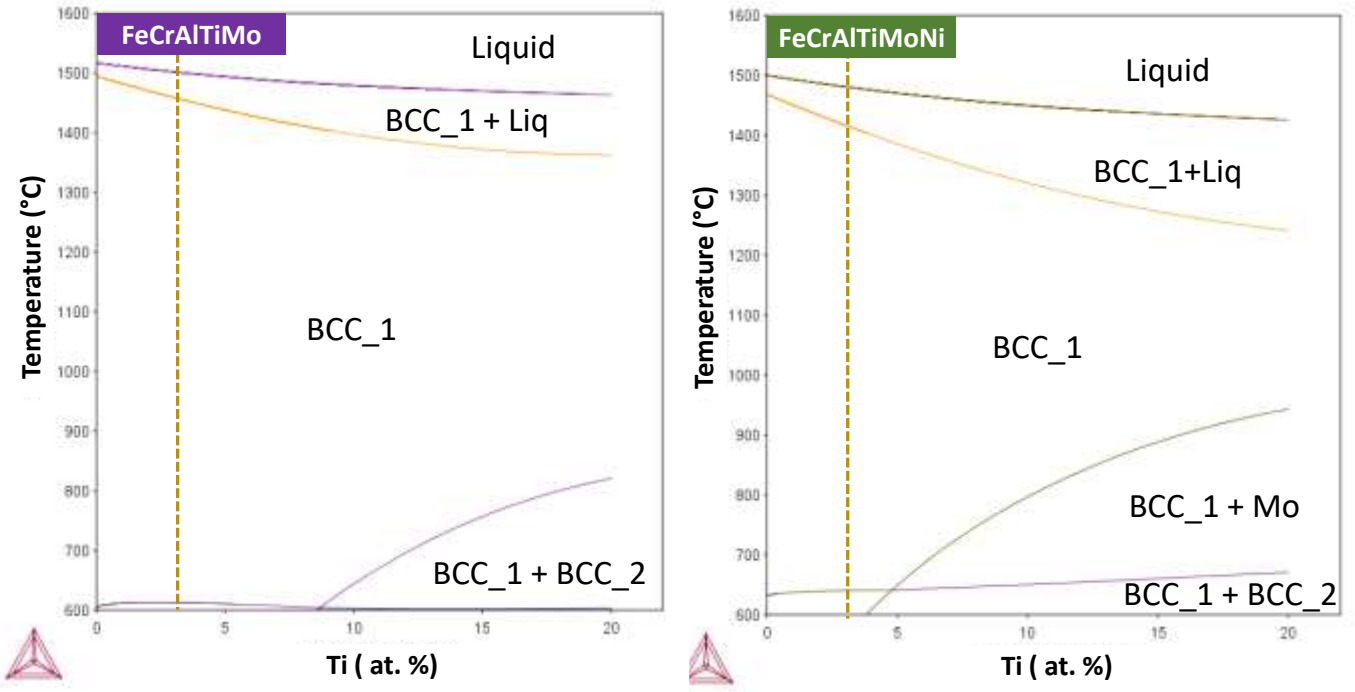

Figure 1. Equilibrium phase diagrams of FeCrAlTiMo (HEA-5) and FeCrAlTiMoNi (HEA-6) calculated by Thermocalc software.

3.2. Validation of HEA new compositions as binder

The design of the three new compositions is validated by their processing by casting. The phase formation of the cast alloys FeCrAlTiMo (HEA-5) and FeCrAlTiMoNi (HEA-6) is studied by XRD and their diffractograms are shown in Figure 2. Both diffractograms show the peaks corresponding with BCC phase although a splitting of peaks is appreciated that may correspond to a decomposition of the BCC phase.

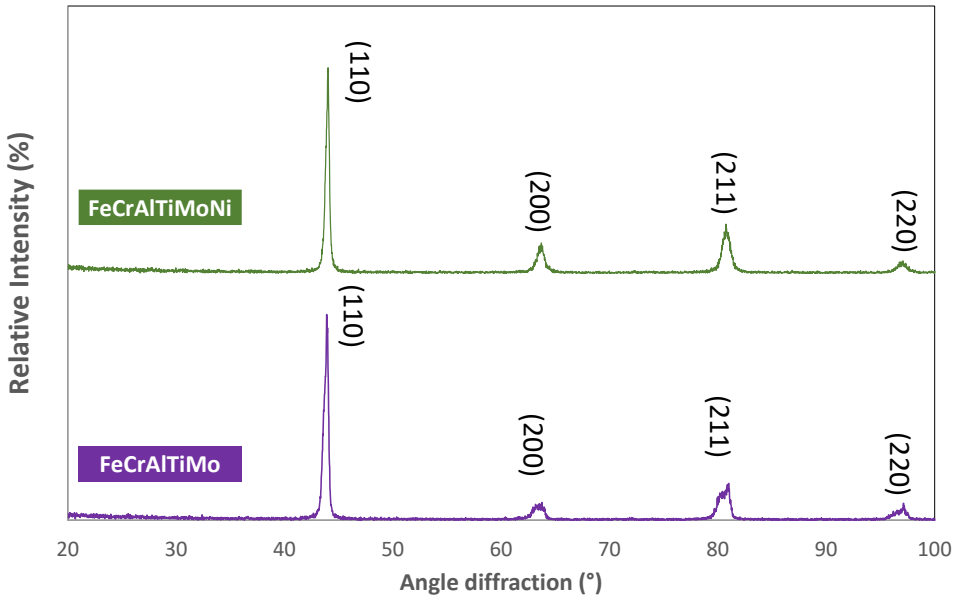

Figure 2. XRD results from cast HEA compositions FeCrAlTiMo (HEA-5) and FeCrAlTiMoNi (HEA-6).

One aspect that must be taken into account when designing compositions that will be used as binder in cermets is the high-temperature interaction between the metallic binder and the hard phase, in this case TiCN. To consider a metallic alloy as a candidate for alternative binder it has to accomplish a good wetting behaviour on TiCN hard phase particles and a partial solubility of TiCN particles in the binder [12]. To study these aspects high temperature wetting experiments have been performed but previously the interaction of the designed alloys with the TiCN hard phase has been studied by calculating their phase diagram and differential thermal analysis. The objective of this study prior to the sintering of the composite material is to understand the phenomena that will occur during sintering to validate a possible future binder. These analyses will allow answering key questions when studying new alloy compositions such as binder in hard materials: what is the melting point of the alloys? How does the presence of carbon influence the thermal behaviour of the alloy? How does the presence of TiCN influence the thermal behaviour of the alloy? Does the presence of hard phase modify the phase formation of the HEA?

In other studied systems (binder alloy)/TiCN a clear influence of the presence of TiCN has been seen in the liquidus temperature of the alloy due to the diffusion of C towards the binder. The influence of the presence of TiCN on the thermal behaviour of HEA-5 and HEA-6 alloys has been studied, as well as the influence of a C content in a similar percentage to that found in TiCN. Thanks to these DTA curves, the sintering temperature that will be used in the consolidation of the two composite materials by SPS can be approximated. The results shown in the heating and cooling curves in differential thermal analysis (DTA) reflect that, as in other candidate alloys to be alternative binder, C decreases the melting point of both HEA-5 and HEA-6 alloy. However, the presence of TiCN does not modify the thermal behaviour of either of the two alloys, contrary to what has been observed in other works with Fe-based binders [3,12].

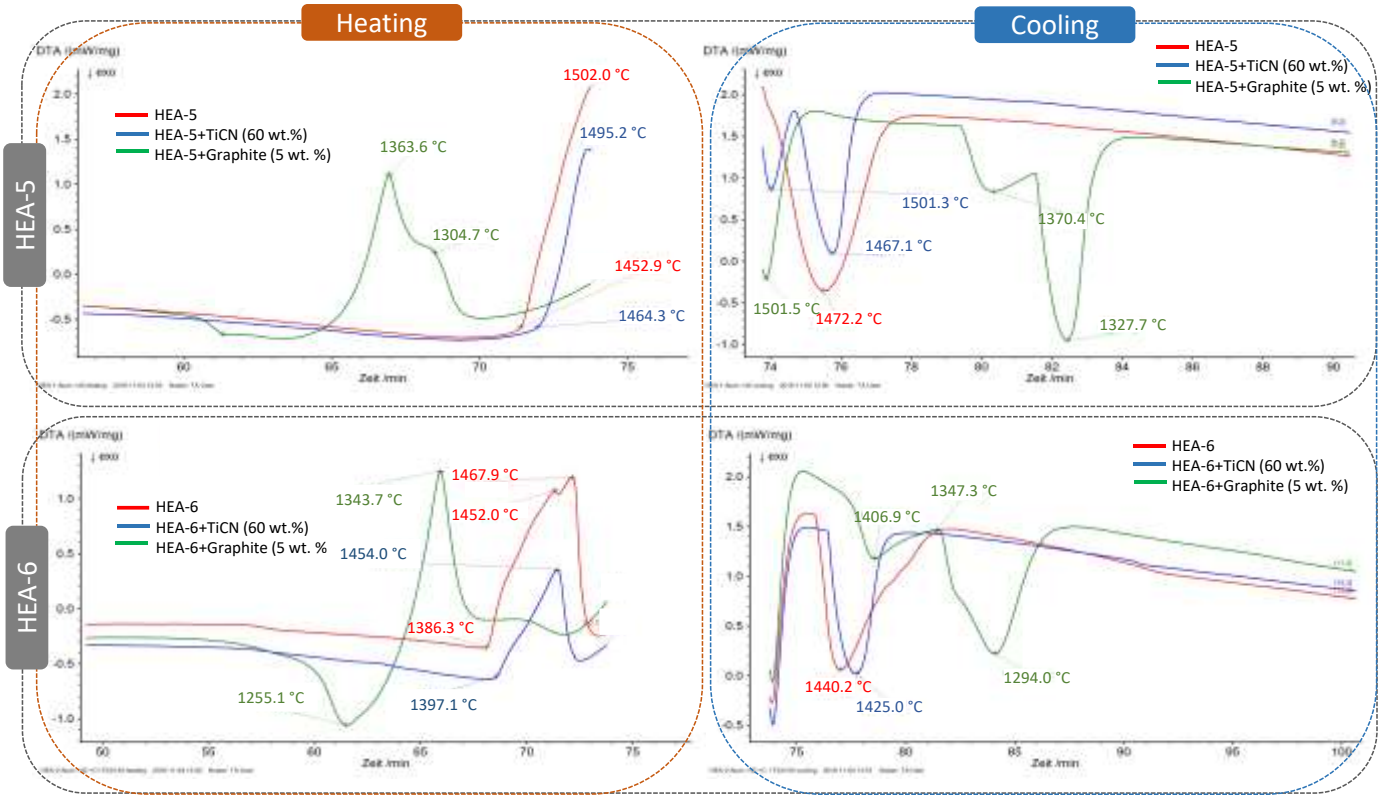

Figure 3. Heating and cooling curves corresponding with Differential Thermal Analysis (DTA) of HEA-5; HEA-5+C; HEA-5+TiCN and HEA-6; HEA-6+C; HEA-6+TiCN.

The calculation of phase diagrams, CALPHAD approach has proven to be very powerful tool to develop cemented carbides and cermets with alternative and new binder compositions [19-27]. In this work the calculation of equilibrium phase diagrams of the designed cermets FeCrAlTiMo (HEA-5)/TiCN and FeCrAlTiMoNi (HEA-6)/TiCN has been performed to study their thermal behaviour and phase formation, both diagrams are shown in Figure 4. Both equilibrium phase diagrams are represented with respect to carbon percentage in the cermet and the composition of the cermet is marked with a vertical dotted line. Looking at the phase diagram of HEA-5/TiCN it can be observed the formation of only one BCC phase and TiCN. Also, the diagram reveals the formation of AlN but in all regions it appears in a percentage lower than 1 mol.%. The diagram of the cermet FeCrAlTiMoNi (HEA-6)/TiCN reveals the formation of the phase AlNi with a B2 crystalline structure in addition to the BCC phase and TiCN.

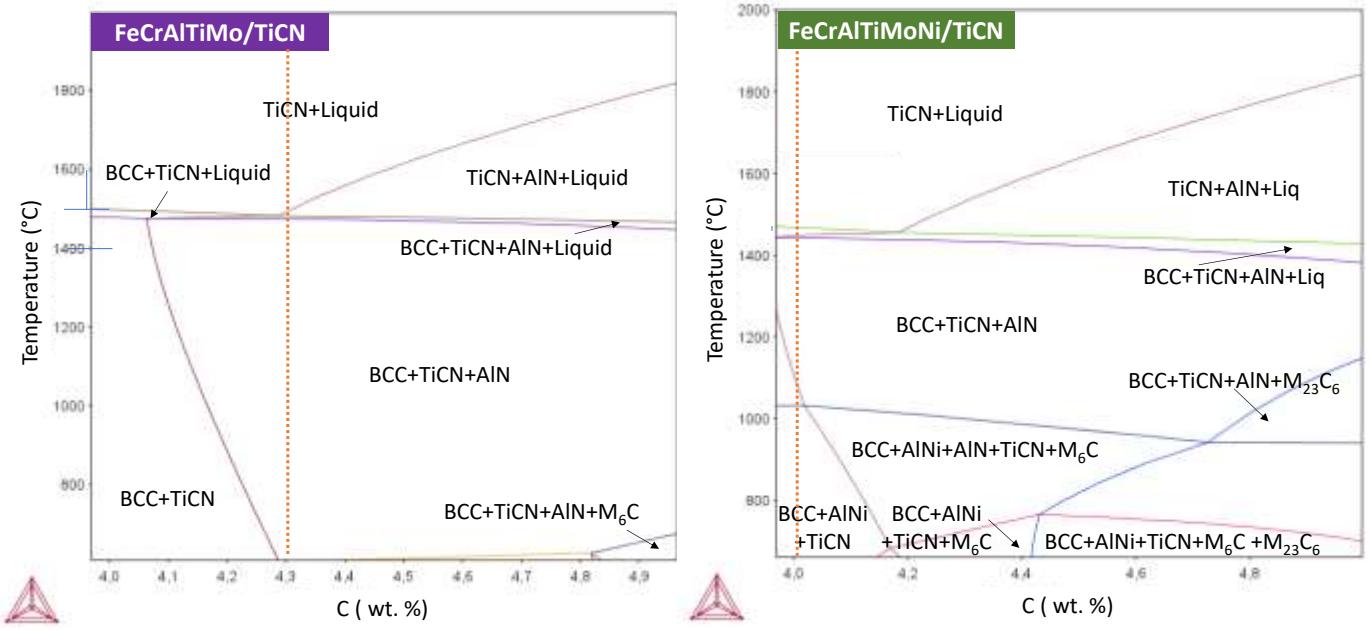

Figure 4. Equilibrium phase diagrams of cermets FeCrAlTiMo (HEA-5)/TiCN and FeCrAlTiMoNi (HEA-6)/TiCN calculated by Thermocalc software.

Table 3 compares the liquidus temperatures of the alloys, HEA-5 and HEA-6, and of the cermets (HEA-5)/TiCN and (HEA-6)/TiCN obtained in the calculated diagrams of Figure 1 and Figure 4 respectively, with their melting points obtained experimentally by means of differential thermal analysis in Figure 3 and very similar values are observed. From which values two conclusions can be drawn: 1) although the calculation of the phase diagrams has been carried out with databases not specific to HEAs, it can be a good approximation tool to predict the thermal behaviour of HEA binder cermets and 2) as has been concluded in the DTA curves, the presence of TiCN does not seem to modify the melting behaviour of the metallic alloy contrary to what has been observed in other metallic alloys used as a binder in cermets [12, 27].

Table 3. Summary of melting points and liquidus temperatures of alloys HEA-5 and HEA-6, and cermets (HEA-5)/TiCN and (HEA-6)/TiCN from Differential Thermal Analysis and Thermocalc phase diagrams.

	Melting point (°C) HEA-5	Liquidus temperature (°C) HEA-5/TiCN	Melting point (°C) HEA-6	Liquidus temperature (°C) HEA-6/TiCN
Differential Thermal Analysis (DTA)	1502.0	1495.2	1467.9	1454.0
Equilibrium phase diagram	1502.0	1500.0	1477.0	1471.0

Once the thermal behaviour of the alloys and the influence of the presence of hard phase are known, the wetting behaviour of the alloys on TiCN is studied by monitoring the evolution of the contact angle between the alloys and the TiCN substrate up to a temperature of 1500 °C and the result of the wetting behaviour when the contact angle stabilizes after the metal melts is shown in Figure 5. In view of the results of the wetting experiments it can be concluded that alloys FeCrAlTiMo (HEA-5) and FeCrAlTiMoNi (HEA-6) show good wetting behaviour on TiCN substrates showing contact angles of θ_{right} = 39 ° and 38°; θ_{left} = 39 ° and 42°, respectively. (It should be noted that low contact angle values are obtained even when the superheat above the melting temperature of the alloys is not very high).

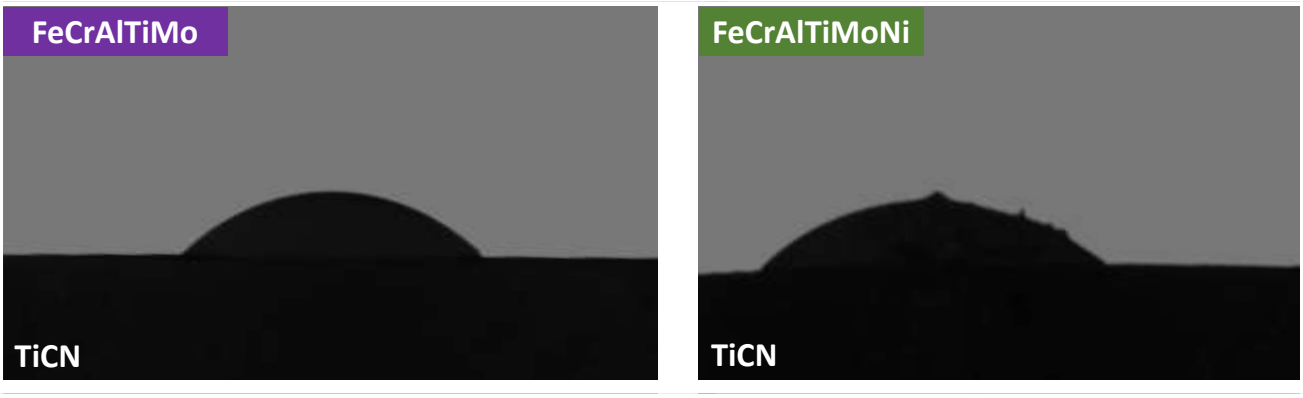

Figure 5. High temperature wetting experiments of FeCrAlTiMo (HEA-5) on a TiCN substrate and FeCrAlTiMoNi (HEA-6) on a TiCN substrate.

The study of the microstructure of transversal surface of the pair HEA/TiCN after wetting experiments allows to know the high temperature interaction between HEA and TiCN. The microstructures of the interface formed in the pair HEA-5/TiCN in Figure 6 reveal the good wetting and solubility of the hard phase TiCN on HEA-5 which is reflected in the presence of the alloy between the grains of the substrate after the experiment. During heating the melted alloy partially dissolves the TiCN substrate and penetrates between the grain of the substrate. This is an important key for the success of the sintering of the future cermet because this good solubility of TiCN will give rise to homogeneous microstructures with a good interface binder/particle. In Figure 7, a detail of the alloy on the TiCN substrate is shown. When analysing the composition of the HEA-5 and the TiCN substrate, the diffusion of C from the substrate to the alloy is observed, in addition to the presence of dark precipitates in the drop formed by the alloy, which compositional analysis reveals that it has precipitated TiCN (note that light element analysis using EDX is qualitative and not quantitative). Furthermore, the compositional analysis shows diffusion of metal elements towards the substrate only at the interface, while at a few microns away from the interface, no diffusion of metal elements towards the substrate is observed. This behaviour in which the solid dissolves in the liquid (and not the other way around) corresponds to

the persistent liquid phase sintering typical of cermets and which gives rise to their typical core-rim microstructure [28].

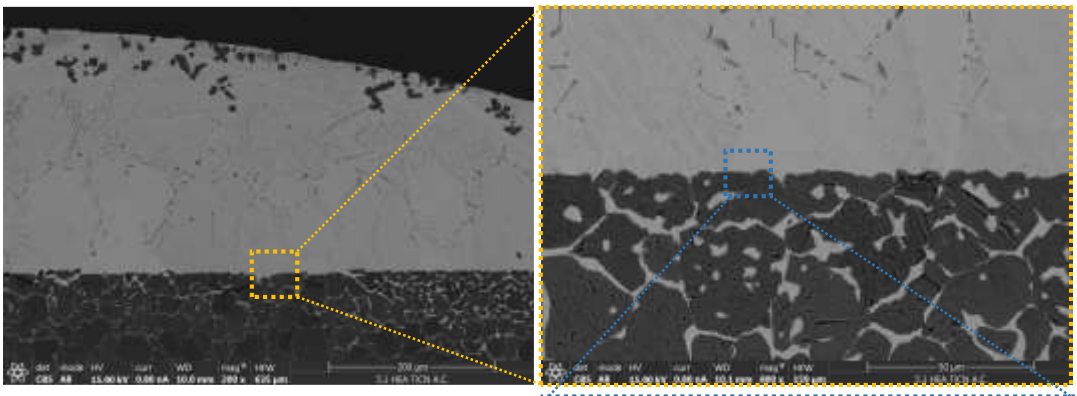

	P1 (wt. %)	P2 (wt. %)	P3 (wt. %)	P4 (wt. %)
C	5.13	8.1	17.92	13.74
N	0.02	0.03	9.58	14.74
Ti	1.35	5.69	53.63	69.33
Al	9.15	8.33	1.52	0.14
Mo	4.9	4.73	2.19	0.28
Cr	28.19	26.35	6.46	0.53
Fe	51.26	46.76	8.7	1.25

Figure 6. Composition and microstructure of the interface formed between HEA-5 and TiCN after wetting experiment.

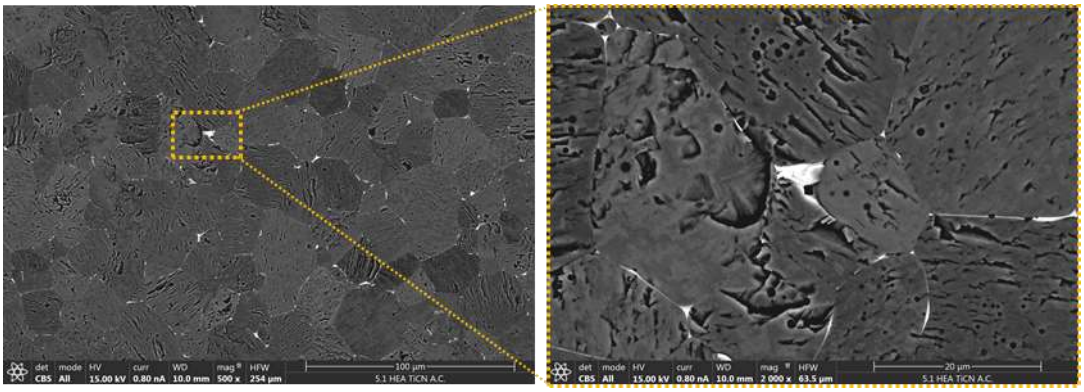

Figure 7. Detail of the infiltration of the molten HEA-5 alloy into TiCN substrate

The study of the interface microstructure formed in the pair HEA-6/TiCN in Figure 8 a and b also reveals a good solubility of the TiCN substrate on the designed alloy with the infiltration of the liquid between the ceramic grains. The compositional analysis does not show a significant elements diffusion, however the microstructure of the alloy in Figure 8a reveals the formation of TiCN precipitates. Taking a closer look, the alloy in Figure 9 shows another type of spherical precipitates. The compositional analysis reveals the formation of a secondary phase rich in Al, Ti and Ni, and not only Al Ni as predicted by the phase diagram (note that the compositional analysis of the precipitates shown is not accurate due to the limited spatial resolution). This phase has also been reported in others compositions of HEAs in the literature with Ni-Al composition [29, 30] showing a crystalline structure B2 type and its presence will influence the mechanical properties of the future cermet. The BCC matrix is a disordered phase while B2 is an ordered phase usually Ni-Al because the formation enthalpy of the binary Al-Ni is more negative and favors the formation of an intermetallic preferentially than a solid solution [31]. In the case of the alloy HEA-6 the binary systems Al-Ni, Ti-Ni and Al-Ti present the lowest values of mixing enthalpy as is shown in Table 4 justifying the B2 (Ti, Al, Ni) formation.

Table 4. Formation enthalpy of binary systems in the alloy FeCrAlMoTiNi.

kJ/mol	Al	Ti	Cr	Fe	Ni	Mo
Al		-30	-10	-11	-22	-5
Ti	-30		-7	-17	-35	-4

Cr	-10	-7		-1	-7	0
Fe	-11	-17	-1		-2	-2
Ni	-22	-35	-7	-2		-7
Mo	-5	-4	0	-2	-7	

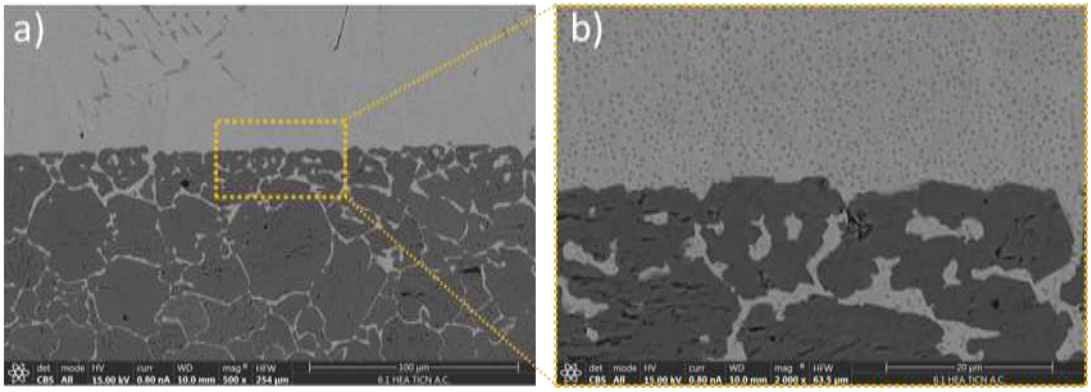

Figure 8. Microstructure of the interface formed between HEA-6 and TiCN after wetting experiment.

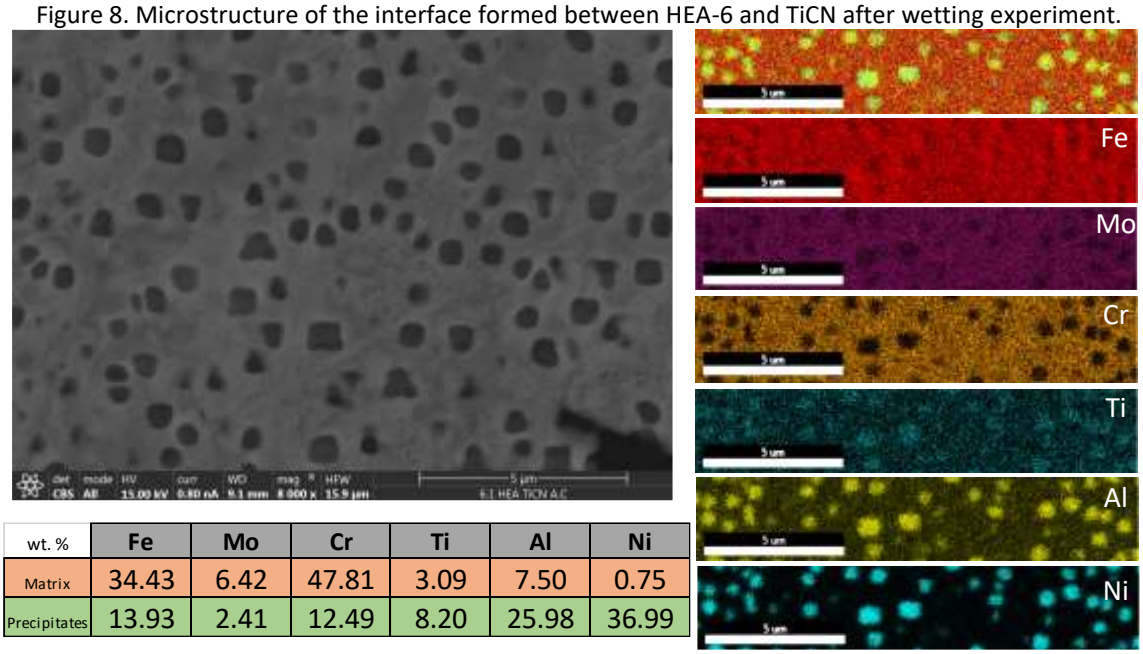

wt. %	Fe	Mo	Cr	Ti	Al	Ni
Matrix	34.43	6.42	47.81	3.09	7.50	0.75
Precipitates	13.93	2.41	12.49	8.20	25.98	36.99

Figure 9. Detail of the microstructure of the alloy HEA-6 formed after wetting experiment.

3.3 Cermets processing

Once the phase formation, the thermal behaviour and the interaction with the TiCN ceramic hard phase of the two designed HEA compositions are known, sintered samples are processed by SPS after the gas atomization of the HEA-5 and HEA-6 powders. The characterization of the atomized powders is presented in the work [x] and reveals an spherical morphology of both HEA-5 and HEA-6 particles, a composition quite similar than the theoretical composition of the designed alloys and a low oxygen content with an experimental density of 6.68 g/cm^3 and 6.72 g/cm^3, respectively.

The microstructures of the sintered samples HEA-5/TiCN and HEA-6/TiCN with relative densities of 98 % and 97 % respectively, are shown in Figure 10 and the diffractograms of both cermets HEA-5/TiCN and HEA-6/TiCN are shown in Figure 11 together with the diffractograms corresponding with the atomized HEA-5 and HEA-6 raw powders and commercial TiCN raw powders. The microstructure of both cermets shows TiCN particles of heterogeneous size and presents the typical core-rim microstructure of these metal ceramic compound materials [32]. In HEA-5/TiCN cermet TiCN core particles presents a composition similar to the stoichiometric TiCN, while the rim presents a composition that shows the presence of elements from metal binder. The composition of the binder is not similar to the theoretical which could mean microstructural changes that require a higher resolution technique to be studied. Difractogram of this cermet shows the peaks corresponding with the hard phase and the peaks corresponding with the BCC although, as in the cast alloys, there is a peaks spliting that could mean a decomposition of the BCC phase. In the analysis of the microstructure of the HEA-6/TiCN cermet it is observed again that the binder has a composition far from the

theoretical of the alloy, however, the AlNi precipitates (B2 phase) found in the alloy after the wetting experiment are not appreciated in the cermet. However, the diffractogram of the cermet HEA6/TiCN in Figure 11 shows a small peak corresponding with the B2 phase therefore, the presence of this second phase in the cermet is not ruled out.

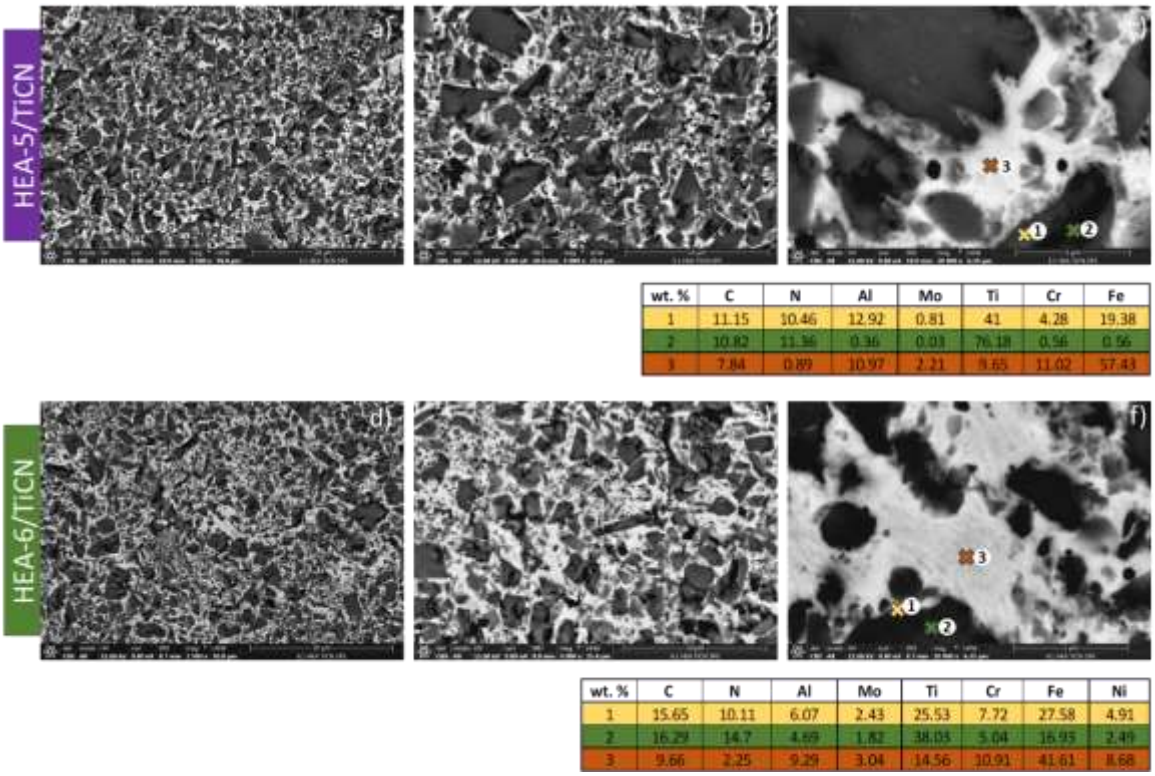

wt. %	C	N	Al	Mo	Ti	Cr	Fe
1	11.15	10.46	12.92	0.81	41	4.28	19.38
2	10.82	11.36	0.36	0.03	76.18	0.56	0.56
3	7.84	0.89	10.97	2.21	8.65	11.02	57.43

wt. %	C	N	Al	Mo	Ti	Cr	Fe	Ni
1	15.65	10.11	6.07	2.43	25.53	7.72	27.58	4.91
2	16.29	14.7	4.69	1.82	38.05	5.04	16.95	2.49
3	9.66	2.25	9.29	3.04	14.56	10.91	41.61	8.68

Figure 10. Microstructures of the sintered cermets by SPS a), b) and c) FeCrAlTiMo (HEA-5)/TiCN d), e) and f) FeCrAlTiMoNi (HEA-6)/TiCN.

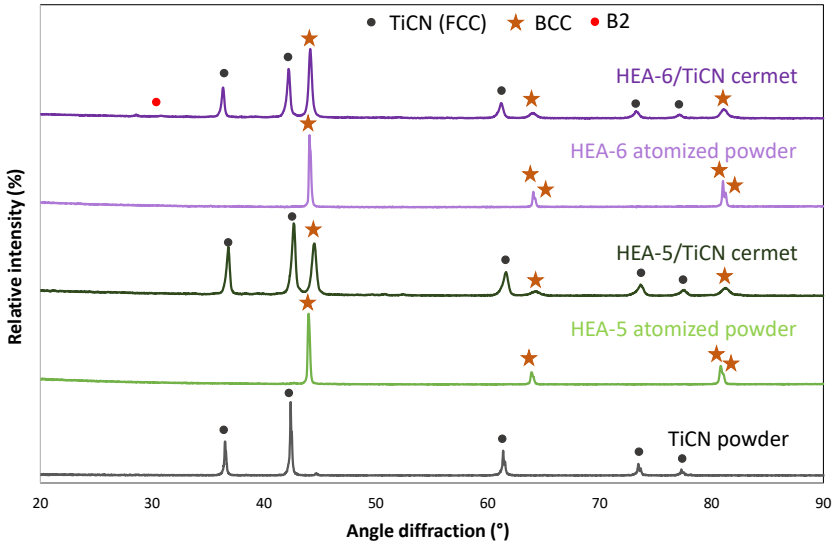

Figure 11. X-Ray diffractograms of the starting powders: TiCN powder, atomized HEA-5 powder and atomized HEA-6 powder and the sintered cermets by SPS FeCrAlTiMo (HEA-5)/TiCN and FeCrAlTiMoNi (HEA-6)/TiCN.

In Figure 12 the engineering stress strain curves after compression test of the cermets HEA-5/TiCN and HEA-6/TiCN are shown. A change in mechanical behaviour is observed in the cermet that has Ni in its composition which shows the formation of the phase B2 in XRD. One of the strategies followed in high entropy alloys to achieve synergy between ductility and strength is the formation of heterogeneities in the microstructure [33]. One of the phases formed for this purpose is the precipitation of coherent ordered B2 in a BCC disordered matrix. The presence of this precipitate is the responsible for the increase in compressive stress shown by the HEA-6/TiCN SPS sample because it acts as an intermetallic but with no detriment to ductility as it is a coherent precipitate [x].

Comparing with the mechanical properties of other cermets, it is observed that the cermet sintered with the alloy HEA-6 as binder presents competitive mechanical properties. When comparing the mechanical properties, the percentage of binder in the composite material must be taken into account. Considering that the two cermets are manufactured with 50 vol. % of binder and the density of the atomized powders is 6.68 g/cm^3 and 6.72 g/cm^3,

respectively, the percentage by weight of binder in the two cermets is 57 wt. %, higher than the usual value in this type of composite materials, so the values of the mechanical properties should be compared taking into account that the cermets presented in other works and here mentioned have 30 wt. % [35] and 11 wt. % [36] of binder. The high percentage of binder in the cermets of this work show high ductility values that may be undesirable for the manufacture of tools because they could lose their shape in service, therefore once the feasibility and perspectives of the HEA designed binders are known the percentage of hard phase in the composite material must be increased in future works.

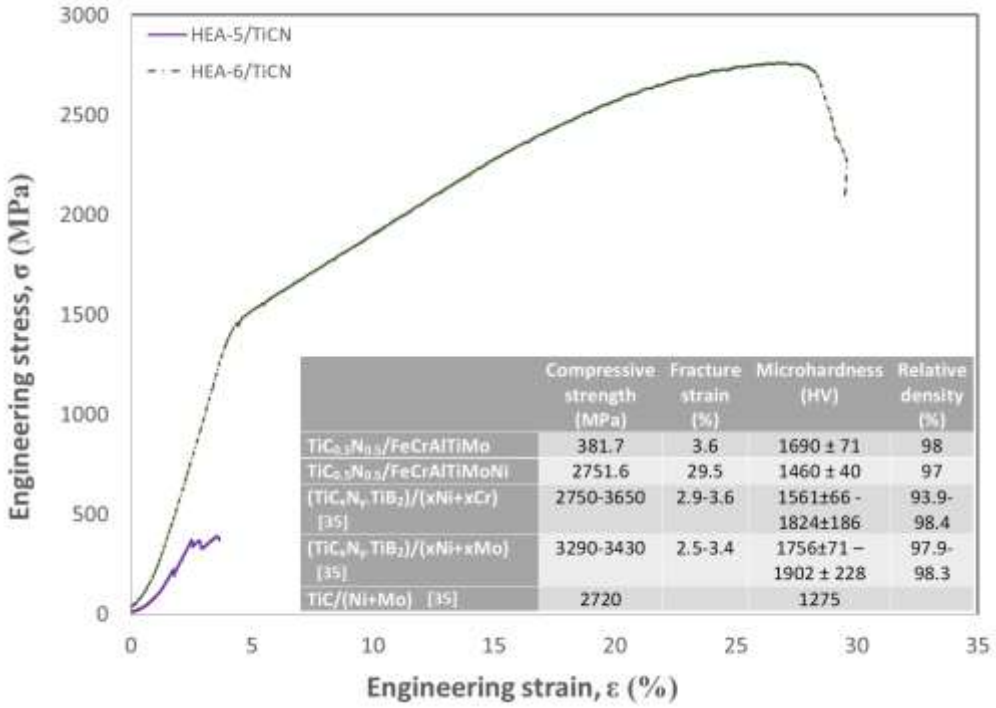

	Compressive strength (MPa)	Fracture strain (%)	Microhardness (HV)	Relative density (%)
$TiC_{0.5}N_{0.5}$/FeCrAlTiMo	381.7	3.6	1690 ± 71	98
$TiC_{0.5}N_{0.5}$/FeCrAlTiMoNi	2751.6	29.5	1460 ± 40	97
(TiC_xN_y, TiB_2)/(xNi+xCr) [35]	2750-3650	2.9-3.6	1561±66 - 1824±186	93.9-98.4
(TiC_xN_y, TiB_2)/(xNi+xMo) [35]	3290-3430	2.5-3.4	1756±71 – 1902 ± 228	97.9-98.3
TiC/(Ni+Mo) [35]	2720		1275	

Figure 12. Compressive curves of cermets HEA-5/TiCN and HEA-6/TiCN. Data comparison with other cermets in the literature.

4. Conclusions

The main objective of this work has been the design of new metallic binder compositions for cermets that have competitive properties compared to cermets with conventional matrices, simplifying the number of phases and compounds present in the composite material. Given the ability to form simple phases of the high entropy alloys, two compositions of these alloys have been designed to study their viability as binder using alloying elements that will presumably provide the properties required in hard materials such as resistance to oxidation and a good combination of mechanical properties HEA-5 and HEA-6. The designed compositions are validated by studying their thermal behaviour and their interaction with the hard phase phase. This study has revealed a good wetting behaviour of the two designed compositions on a TiCN substrate and it has been seen that the presence of TiCN does not alter the thermal behaviour of the alloys, contrary to what occurs with other iron-based alloys studied.

The study of the mechanical behaviour of sintered cermet has revealed a considerable improvement in terms of fracture strain and compressive strength when the composition of the binder has Ni, the reason being the separation of BCC-B2 phases that allows a good balance between mechanical properties.

As a final idea, it is highlighted that this first study of the new composition of high entropy alloys such as binder have allowed obtaining a cermet with competitive properties with other conventional binder cermets, reducing the amount of critical elements in terms of toxicity and price, the density of the composite material and the number of phases present, which make this new cermet a promising material and a candidate composition for further investigation.

5. Bibliography

[1] S. Norgren, J. Garcia, A. Blomqvist, L. Yin, Trends in the P/M hard metal industry, Int. J. Refract. Met. Hard Mater. 48 (2015) 31–45.

[2] J. Kübarsepp, K. Juhani. Cermets with Fe-alloy binder: A review. Int. J. Refract. Met. Hard Mater. 92 (2020) 105290.
[3] M. de Nicolas, H. Besharatloo, P. Alvaredo, J.J. Roa, L. Llanes, E. Gordo, Design of alternative binders for hard materials, Int. J. Refract. Met. Hard Mater. 87 (2020) 105089.
[4] P. Alvaredo, J. Escribano, B. Ferrari, A.J. Sanchez-Herencia, E. Gordo, Steel binder cermets processed by combination of colloidal processing and powder metallurgy. Int. J. Refract. Met. Hard Mater. 74 (2018) 1-6.
[5] Y. Shao, Z. Guo, Y. Wang, H. Ma. Fabrication and characterization of NbC-CoCrFeNiMn high entropy alloy cermets. Int. J. Refract. Met. Hard Mater. 94 (2021) 105388.
[6] Q. Gou, J. Xiong, Z. Guo, J. Liu, L. Yang, X. Li. Influence of NbC additions on microstructure and wear resistance of Ti(C,N)-based cermets bonded by CoCrFeNi high-entropy alloy. Int. J. Refract. Met. Hard Mater. 94 (2021) 105375.
[7] Y. Fang, N. Chen, G. Du, M. Zhang, X. Zhao, H. Cheng, J. Wu. The microstructure and properties of novel Ti(C,N)-based cermets with multicomponent CoCrFeNiCu high-entropy alloy binders. J. Alloys Compd. 815 (2020) 152486
[8] A. G. de la Obra, M. J. Sayagués, E. Chicardi, F. J. Gotor. Development of Ti(C,N)-based high entropy alloys as binder phase. J. Alloys Compd. 814 (2020) 152218.
[9] Z. Li, X. Liu, K. Guo, H. Wang, F. Chang, C. Hong, P. Dai, Microstructure and properties of Ti(C,N)-TiB2 FeCoCrNiAl high-entropy alloys composite cermets. Mater. Sci. Eng. A. 767 (2019) 138427
[10] B. Cantor, I.T.H. Chang, P. Knight, A. J. B. Vincent. Microstructure development in equiatomic multicomponent alloys. Mater. Sci. Eng. A 375 (2004) 213–218.
[11] X. Chang, M. Zeng, K. Liu, L. Fu. Phase engineering of High-Entropy Alloys. Adv. Mater. 21 (2020) 1907226
[12] P. Alvaredo. M. Dios, B. Ferrari, E. Gordo. Understanding of wetting and solubility behaviour of Fe binder on Ti(C,N) cermets. J. Alloys Compd. 770 (2019) 17-25.
[13] P. Alvaredo, E. Gordo, O. Van der Biest, K. Vanmeensel. Microstructural development and mechanical properties of iron based cermets processed by presureless and spark plasma sintering. Mater. Sci. Eng. A 538 (2012) 28-34
[14] P. Alvaredo, S. A. Tsipas, E. Gordo. Influence of carbon content on the sinterability of an FeCr matrix cermets reinforced with TiCN. Int. J. Refract. Hard Mat. 36 (2013) 283-288
[15] S. Guo, C. T. Liu. Phase stability in high entropy alloys: formation of solid-solution phase or amorphous phase. Pro. Nat. Sci-Mater., 21 (2011) 433-446.
[16] F. Tian, L. K. Varga, N. Chen, J. Shen, L. Vitos. Empirical design of single phase high-entropy alloys with high hardness. Intermetallics, 58 (2015) 1-6.
[17] L. Jiang, Y. P. Lu, H. Jiang, T. M. Wang, B. N. Wei, Z. Q. Zao, T. J. Li. Formation rules of single phase solid solution in high entropy alloys. Mater. Sci. Technol., 32-6 (2016) 588-592.
[18] M. Calvo-Dahlborg, S. G. R. Brown. Hume-Rothery for HEA classification and self-organizing map for phases and properties prediction. J. Alloys Compd., 724 (2017) 353-364.
[19] A.F. Guillermet, An assessment of the Fe-Ni-W-C phase diagram, Metallkunde. 78 (1987) 165 – 170.
[20] A.F. Guillermet, Use of phase diagram calculations in selecting the composition of Fe-Ni bonded WC tools, Int. J. Refract. Hard Mat. 6 (1987) 24-27.
[21] B. Uhrenius, Phase diagrams as a tool for production and development of cemented carbides and steels, Powder Metall. 35 (1992) 203-210.
[22] B. Uhrenius, H. Pastor, E. Pauty, F.G. Cedex, On the composition of Fe-Ni-Co-WC-based cemented carbides, 15 (1997) 139-149.
[23] P. Zhou, Y. Peng, C. Buchegger, Y. Du, W. Lengauer, Experimental investigation and thermodynamic assessment of the C-Co-Fe-Ni-W system, Int. J. Refract. Met. Hard Mater. 54 (2016) 60-69.
[24] S.G. Huang, J. Vleugels, H. Mohrbacher, M. Woydt, Microstructure and mechanical properties of NbC matrix cermets using Ni containing metal binder, Met. Powder Rep. 71 (2016) 349 – 355
[25] S. Norgren, J. García, On gradient formation in alternative binder cemented carbides, Int. J. Refract. Met. Hard Mater. 73 (2018) 106 – 110.
[26] R. De Oro, A. Agna, U. Umbelino, W.-D. Schubert, Phase formation in cemented carbides prepared from WC and stainless steel powder – An experimental study combined with thermodynamic calculations, Int. J. Refract. Metals Hard Mater. 80 (2019) 225 – 237.
[27] P. Alvaredo, P. Bruna, D. Crespo, E. Gordo. Influence of carbon content on microstructure and properties of a steel matrix cermet. Int. J. Refract. Met. Hard Mater. 75 (2018) 78-84.
[28] S. Ahn, S. Kang. Formation of Core/Rim Structures in Ti(C,N)-WC-Ni Cermets via a Dissolution and Precipitation Process. J. Am. Ceram. Soc. 83 (2000) 1489-94

[29] V. Soni, O. N. Senkov, B. Gwalani, D. B. Miracle, R. Banerjee. Microstructural design for improving ductility of an initially brittle refractory high entropy alloy. Sci. Rep., 8 (2018) 8816.
[30] L. Lin, X. Xian, Z. Zhong, Y. Wu, P. K. Liaw. Microstructure stability and its influence on the mechanical properties of $CrMnFeCoNiAl_{0.25}$ high entropy alloy. Met. Mater. Int. 26 (2020) 1192-1199.
[31] F. Otto, Y. Yang, H. Bei, E.P. George. Relative effects of enthalpy and entropy on the phase stability of equiatomic high- entropy alloys. Acta Mater. 61 (2013) 2628-2638.
[32] L. Chen, W. Lengauer, K. Dreyer. Advances in modern nitrogen-containing hardmetals and cermets. Int. J. Refract. Met. Hard Mater. 18 (2000) 153-161.
[33] E. Ma, X. Wu. Tailoring heterogeneities in high entropy alloys to promote strength-ductility synergy. Nat. Commun. (2019) 10:5623.
[34] Y. Ma, B. Jiang, C. Li, Q. Wang, C. Dong, P. K. Liaw, F. Xu, L. Sun. The BCC/B2 morphologies in AlxNiCoFeCr high-entropy alloys. Metals (2017) 7, 57
[35] F. Chang, F. Qiu, C. Li, Y. Wang, Q. Jiang. Effects of Cr and Mo elements on the microstructures and compressive properties of the in situ (TiCxNy-TiB2)/Ni cermets. Prog. Nat. Sci. 29-1 (2019) 20-27.
[36] S. R. Agnew, L. D. Jasmine, I. K. Haydn, N. G. Wadley. Mechanical properties of large TiC-Mo-Ni cermet tiles. Int. J. Refract. Met. Hard Mater. 75 (2018) 238-247